*Original Research*

# Toward improved myocardial maturity in an organ-on-chip platform with immature cardiac myocytes

**Sean P Sheehy[1], Anna Grosberg[1], Pu Qin[2], David J Behm[2], John P Ferrier[1], Mackenzie A Eagleson[1], Alexander P Nesmith[1], David Krull[3], James G Falls[3], Patrick H Campbell[1], Megan L McCain[1], Robert N Willette[2], Erding Hu[2] and Kevin K Parker[1]**

[1]Disease Biophysics Group, Wyss Institute for Biologically Inspired Engineering, Harvard Stem Cell Institute, and John A. Paulson School of Engineering and Applied Sciences, Harvard University, Cambridge, MA 02138, USA; [2]Heart Failure Discovery Performance Unit, Metabolic Pathways and Cardiovascular Therapy Area Unit, GlaxoSmithKline Pharmaceuticals, King of Prussia, PA 19406, USA; [3]Safety Assessment Unit, GlaxoSmithKline Pharmaceuticals, King of Prussia, PA 19406, USA
Corresponding author: Kevin K Parker. Email: kkparker@seas.harvard.edu

Impact statement

With the recent focus on developing *in vitro* Organ-on-Chip platforms that recapitulate tissue and organ-level physiology using immature cells derived from stem cell sources, there is a strong need to assess the ability of these engineered tissues to adopt a mature phenotype. In the present study, we compared and contrasted engineered tissues fabricated from neonatal rat ventricular myocytes in a Heart-on-a-Chip platform to ventricular muscle strips isolated from adult rats. The results of this study support the notion that engineered tissues fabricated from immature cells have the potential to mimic mature tissues in an Organ-on-Chip platform.

## Abstract

*In vitro* studies of cardiac physiology and drug response have traditionally been performed on individual isolated cardiomyocytes or isotropic monolayers of cells that may not mimic desired physiological traits of the laminar adult myocardium. Recent studies have reported a number of advances to Heart-on-a-Chip platforms for the fabrication of more sophisticated engineered myocardium, but cardiomyocyte immaturity remains a challenge. In the anisotropic musculature of the heart, interactions between cardiac myocytes, the extracellular matrix (ECM), and neighboring cells give rise to changes in cell shape and tissue architecture that have been implicated in both development and disease. We hypothesized that engineered myocardium fabricated from cardiac myocytes cultured *in vitro* could mimic the physiological characteristics and gene expression profile of adult heart muscle. To test this hypothesis, we fabricated engineered myocardium comprised of neonatal rat ventricular myocytes with laminar architectures reminiscent of that observed in the mature heart and compared their sarcomere organization, contractile performance characteristics, and cardiac gene expression profile to that of isolated adult rat ventricular muscle strips. We found that anisotropic engineered myocardium demonstrated a similar degree of global sarcomere alignment, contractile stress output, and inotropic concentration–response to the β-adrenergic agonist isoproterenol. Moreover, the anisotropic engineered myocardium exhibited comparable myofibril related gene expression to muscle strips isolated from adult rat ventricular tissue. These results suggest that tissue architecture serves an important developmental cue for building *in vitro* model systems of the myocardium that could potentially recapitulate the physiological characteristics of the adult heart.

**Keywords:** Muscular thin films, cardiac contractility, Heart-on-a-Chip, cardiac tissue engineering

***Experimental Biology and Medicine* 2017; 242: 1643–1656. DOI: 10.1177/1535370217701006**

## Introduction

For over a century, myocytes isolated from the heart have been used to study cardiac physiology.[1] However, these studies have largely relied on immature cells grown in an isotropic configuration that do not accurately recapitulate *in vivo* tissue function and drug response.[2] Thus, one of the primary goals in the field of cardiac tissue engineering is to identify and develop techniques for promoting the maturation of engineered cardiac tissues *in vitro*.[3–5] In recent years, a number of *in vitro* platforms have been proposed to generate engineered myocardial tissues from a variety of cell sources, including human stem cell-derived cardiomyocytes, which facilitate study of myocardial function and pharmacological response profile.[6–10] These platforms employed a number of strategies to recapitulate the three-dimensional architecture of muscle tissue by relying on the self-assembly of cardiomyocytes in an ECM hydrogel and utilizing biomechanical loading to promote maturation

*in vitro*.[6,7,11–13] While these platforms allowed successful measurement of inotropic response to pharmacological agents, further study is needed to determine how closely engineered myocardial tissues match their native counterpart and to identify the most effective set of microenvironmental cues for driving myocardial maturation *in vitro*. It has long been postulated that physical and mechanical microenvironmental cues play an important role in the development of a number of organ systems, including the heart.[14–16] As the heart develops, cardiac myocytes undergo a number of morphological changes as they progress toward the adult phenotype,[17–19] and self-organize into laminar sheets of muscle tissue.[18,20,21] Dynamic remodeling of the actin cytoskeleton in localized regions of cardiac myocytes has been implicated in causing changes in cell shape that drive looping of the heart tube during embryonic development, supporting a role for remodeling at the scale of the cytoskeleton to influence architectural features at the tissue scale.[22–25] Moreover, mechanical interactions between cardiac myocytes and the extracellular matrix (ECM), or between cardiac myocytes and neighboring cells form a mechanosensory circuit with the cytoskeleton and intracellular signaling machinery that has been implicated in influencing a number of functional characteristics, including impulse propagation,[26,27] contractile force output,[21] and excitation–contraction coupling.[28] Under pathological conditions, this mechanotransduction signaling paradigm allows the cytoskeleton to remodel in response to alterations in the load on the myocardium, such that the aspect ratio and sarcomere density of cardiac myocytes are reconfigured in an attempt to maintain cardiac output, further supporting a role for cytoskeletal architecture in mediating intracellular biological responses to extracellular mechanical cues.[14,19,26,29] These findings highlight the importance of cell shape and tissue architecture in the functional development of the heart and suggest that controlling cell shape could serve as a vital cue for building accurate models of the myocardium *in vitro*.[30]

*In vitro* studies of this interrelationship between cell shape and biological function have been made possible by the development of techniques, such as micro-contact printed ECM[31,32] and the introduction of micro-grooves into cell culture substrates[33,34] that provide extracellular boundary conditions. Initial studies of neonatal rat cardiac myocytes cultured on micro-contact printed ECM substrates provided the first insights into the relationship between myocardial tissue architecture and electrical impulse propagation.[32,35,36] Further studies using micro-contact printed ECM substrates have shown that geometric guidance cues can be used to predictably[37] and reliably[38] direct the assembly of the contractile apparatus in cultured cardiac myocytes. The boundary conditions presented by patterned ECM proteins were found to guide the assembly and parallel bundling of the actin cytoskeletal network as sarcomerogenesis proceeded, such that nascent sarcomeres would adopt uniaxial alignment along the long axis of the cardiac myocyte if a rectangular aspect ratio was presented.[38] Further, it has been shown that in addition to directing sarcomerogenesis, myocyte shape also influences $Ca^{2+}$ transient dynamics,[39,40] electrical activity,[41] and contractile force generation[39,42] at both the single cell and tissue level. Isolated ventricular myocytes cultured on patterned fibronectin (FN) substrates designed to recapitulate the anisotropy of the myocardium self-organized into tissues with highly aligned sarcomeres and substantially greater contractile force output than cardiac myocytes cultured on uniform layers of FN that allowed random cellular organization.[41] The results of these studies clearly demonstrated a role for cell shape and tissue organization in modulating the myofibril architecture and functional performance of engineered myocardium. However, it is unclear what effect these cues may have on cardiac gene expression, and how closely these engineered heart muscle constructs recapitulate the physiological characteristics of the *in vivo* myocardium.

We hypothesized that directing the self-assembly of isolated cardiac myocytes into anisotropic sheets of muscle using ECM guidance cues promotes maturation of engineered myocardium toward the adult myocardial phenotype by influencing cardiac gene expression, in addition to controlling tissue architecture. To test this hypothesis, we cultured neonatal rat ventricular myocytes on micro-contact printed lines of FN designed to mimic the laminar architecture of the *in vivo* myocardium and measured sarcomere alignment, cardiac gene expression, auxotonic contraction, and inotropic response to the β-adrenergic agonist, isoproterenol. We then measured these same physiological parameters in explants of the adult rat ventricular myocardium and contrasted the results to those observed in the engineered myocardium. We found that anisotropic engineered myocardium exhibited values that approached those observed in the adult rat myocardium for the set of physiological parameters tested. These results suggest that the mechanical signaling cascades that are activated by dynamic regulation of cytoskeletal architecture during heart development could be activated *in vitro* using extracellular boundary conditions encoded in the ECM as part of a larger strategy to fabricate engineered myocardium with adult-like structural and functional characteristics.

## Materials and methods

### Ethics statement

All procedures involving the isolation of rat cells and tissues used in this study were carried out in accordance with recommendations included in the NIH Guide for the care and use of laboratory animals. Procedures performed at Harvard University were approved by the Harvard University Institutional Animal Care and Use Committee (IACUC) under Animal Experimentation Protocol number 24-01 entitled ''Harvest and Culture of Neural and Cardiac Tissue from Neonatal Rats and Mice for *In Vitro* Disease Models'' to ensure that they meet the standards set by the Faculty of Arts and Sciences at Harvard University for the use of vertebrate animals in research and teaching. Procedures performed at GlaxoSmithKline were reviewed and approved by the IACUC at GlaxoSmithKline under protocol number PA0336 and conducted in accordance with the GlaxoSmithKline Policy on the Care, Welfare and Treatment of Laboratory Animals.

### Muscular thin film (MTF) substrate fabrication

Glass coverslips were masked using adhesive tape to cover all but a 6 mm × 18 mm rectangle in the center of the coverslip, then spin coated with a thermo-sensitive sacrificial polymer, Poly(*N*-isopropylacrylamide) (PiPAAm, Polysciences, Inc., Warrington, PA). Subsequently, a layer of polydimethylsiloxane (PDMS) was spin coated over the PiPAAm layer and cured at 65°C overnight. The thickness of the PDMS layer was determined to be in the range of 10–18 μm for all MTF cantilevers used in this study using a stylus profilometer (Dektak 6M, Veeco Instruments Inc., Plainview, NY). MTF cantilevers were cut from the PDMS layer either by hand using a straight-blade razor or using a $CO_2$ laser (Epilog, Golden, CO) to create an array of 4–8 rectangular films over the PiPAAm area of the chip. Typical dimensions of the MTF cantilevers were 1–2 mm in width, 2–5 mm in length, and were separated by 0.5–1 mm spacing.

### Micro-contact printing geometrically defined ECM patterns

Silicone stamps designed for micro-contact printing linear arrays of ECM protein were prepared as previously described,[38,41] with slight modifications to the patterns used to fabricate anisotropic tissues. Previously, 20 μm wide FN lines spaced 20 μm apart were used to direct the self-assembly of cardiac myocytes into aligned tissues,[41] but recent work has shown that 15 μm wide FN lines provide improved cellular alignment, and that reducing the spacing between the FN lines from 20 to 2 μm allows the formation of aligned muscle sheets without the need to backfill the spaces between the micro-contact printed lines with a lower concentration of FN protein.[9] Thus, photolithography masks with grids of 15 μm wide lines spaced either 2 or 15 μm apart were designed using Autocad software (Autodesk, San Rafael, CA) and used to prepare silicon wafers with negatives of the patterns for replica molding. Sylgard 184 PDMS (Dow Corning, Midland, MI) was poured over the replica molding wafers, degassed in a vacuum chamber for 1 h, and cured at 60°C overnight. Glass coverslips were spin coated with PDMS and UV-ozone cleaned (Jelight Company, Inc., Irvine, CA) for 8 min just before stamping. Immediately prior to ECM pattern transfer to PDMS-coated coverslips, stamps were incubated for 1 h with a solution of 50 μg/mL of the ECM protein FN (BD Biosciences, Bedford, MA). After transfer of the FN pattern to the surface of the PDMS-coated coverslips, they were incubated in 1% (w/v) Pluronic F127 (BASF, Ludwigshafen, Germany) for 15 min to block cell adhesion to unstamped regions, and rinsed three times with sterile phosphate-buffered saline (PBS).

### Neonatal rat ventricular myocyte isolation and culture

Ventricular tissue was isolated from two-day old Sprague Dawley rats (Charles River Laboratories, Wilmington, MA) in accordance with procedures approved by the Harvard University IACUC. Briefly, neonatal rats were euthanized via decapitation and ventricular tissue excised through a midsternal incision. Isolated ventricular tissue was dissociated into single cells via incubation in a 0.1% (w/v) trypsin solution (USB Corp., Cleveland, OH) with mechanical agitation at 4°C for 12 h, followed by four serial incubations in a 0.1% (w/v) solution of collagenase type II (Worthington Biochemical, Lakewood, NJ) at 37°C for 2 min each. Following dissociation, cell solutions were subjected to two serial preplating steps in T175 culture flasks for 45 min each to enrich the cardiac myocyte population. Isolated cardiac myocytes were seeded onto MTF substrates with micro-contact printed FN ECM patterns at a density of 100,000 cells/cm$^2$ and maintained in a culture medium consisting of Medium 199 (Invitrogen, Carlsbad, CA) supplemented with 10% (v/v) heat-inactivated fetal bovine serum (FBS), 10 mM HEPES, 20 mM glucose, 2 mM L-glutamine, 1.5 μM vitamin B-12, and 50 U/mL. The amount of FBS in the culture medium was reduced to 2% (v/v) from the second day of culture onward to limit non-myocyte proliferation, and medium was exchanged every 48 h thereafter.

### MTF contractility measurements

For measurement of contractile force generation by engineered cardiac tissues, MTF chips were transferred to a stereomicroscope with darkfield base, (Leica Microsystems Inc., Wetzlar, Germany) in a 60 mm Petri dish filled with a normal Tyrode's solution (mM, 5.0 HEPES, 5.0 glucose, 1.8 $CaCl_2$, 1.0 $MgCl_2$, 5.4 KCl, 135.0 NaCl, and 0.33 $NaH_2PO_4$; reagents from Sigma Aldrich, St. Louis, MO) at 37°C. Bath temperature was allowed to drop below the PiPAAm transition temperature to release the free edges of the cantilevers from the glass coverslip and allow the MTFs to bend away from the glass as the engineered tissues contracted. Video recordings of MTF length (prior to peeling the films off) and x-projection as cardiac tissues contracted were taken at 100 fps using a high-speed CCD camera (A602f Basler Inc, Exton, PA) controlled by LabView (National Instruments, Austin, TX). During recordings, engineered cardiac tissues were paced at 2 Hz (5–10 V, 10 ms pulse) using an external field stimulator (Myopacer, IonOptix Corp., Milton, MA) in a temperature-controlled bath (34–37°C) throughout the experiment.

The stress produced by engineered cardiac tissues was calculated from the radius of curvature produced by bending of the MTFs as previously described.[43,44] The length ($L$) and x-projection of the MTFs ($x$) was measured using custom image processing software. The radius of curvature was numerically calculated according to

$$x = \begin{cases} r\sin\left(\frac{L}{r}\right) \Rightarrow \frac{2L}{\pi} < x < L \\ r \Rightarrow \frac{L}{2\pi} < x < \frac{2L}{\pi} \end{cases} \quad (1)$$

The radius of curvature and thickness of the PDMS layer of the MTF were input for every film and analyzed using a custom script written in MatLab (Mathworks, Natick, MA) to calculate the stress according to a volumetric growth method.[45,46] The systolic and diastolic stresses were calculated as the average of the maxima and minima in the oscillating stress trace, respectively. The active stress was calculated as the difference between the systolic and diastolic stresses.

### Immunohistochemical staining

Samples were fixed in 4% (v/v) paraformaldehyde with 0.05% (v/v) Triton X-100 in PBS at room temperature for 10 min, followed by three rinses in room temperature PBS. Then, samples were incubated in a primary antibody solution consisting of 1:200 dilutions of monoclonal antisarcomeric α-actinin antibody (A7811, clone EA-53, Sigma Aldrich, St. Louis, MO), polyclonal anti-FN antibody (F3648, Sigma-Aldrich, St. Louis, MO), 4′,6′-diamidino-2-phenylindole hydrochloride (Invitrogen, Carlsbad, CA), and Alexa Fluor 633-conjugated phalloidin (Invitrogen, Carlsbad, CA) for 1 h at room temperature. Samples were then rinsed three times in room temperature PBS and incubated in 1:200 dilutions of Alexa Fluor 488-conjugated goat anti-mouse IgG and Alexa Fluor 546-conjugated goat anti-rabbit IgG secondary antibodies (Invitrogen, Carlsbad, CA) for 1 h at room temperature. Fluorescence imaging was performed using a Zeiss LSM confocal microscope (Carl Zeiss Microscopy, Jena, Germany).

### Quantitative assessment of sarcomere organization

Fluorescence images of sarcomeric α-actinin in immunohistochemically labeled engineered cardiac tissues were used to assess global z-line organization with custom software implemented in ImageJ (NIH, Bethesda, MD) and Matlab (Mathworks, Natick, MA) that utilize previously described algorithms[41] and improve upon their ability to distinguish α-actinin associated pixels from image noise.[47] Briefly, sarcomere orientation ($\vec{r} = [r_i, r_j]$) at every pixel was calculated using a ridge detection algorithm.[48] The orientational order parameter (OOP) was calculated as the maximum eigenvalue of the following tensor

$$\overline{\overline{T}} = \left\langle 2\begin{bmatrix} r_i r_i & r_i r_j \\ r_i r_j & r_j r_j \end{bmatrix} - \begin{bmatrix} 1 & 0 \\ 0 & 1 \end{bmatrix} \right\rangle \quad (2)$$

The OOP ranges from zero for isotropic systems to one for perfectly aligned systems[49,50] and was used as a metric for global sarcomere organization in engineered tissues, with values approaching one indicating a high degree of parallel sarcomere alignment throughout the tissue, and values approaching zero representing tissues with more random sarcomere alignment.

### RT-qPCR gene expression measurements

Total RNA was collected in triplicate from both isotropic and micropatterned anisotropic samples using a Stratagene Absolutely RNA Miniprep kit (Agilent Technologies, Santa Clara, CA) according to the manufacturer's instructions and in triplicate from three-month-old Sprague Dawley rat ventricular tissue using an RNeasy mini fibrous tissue kit (Qiagen Inc, Valencia, CA). Genomic DNA contamination was eliminated by incubating the RNA lysates in DNase I digestion buffer at 37°C for 15 min during the RNA purification procedure. The quantity and purity of RNA lysates was assessed using a Nanodrop spectrophotometer (Thermo Scientific, Wilmington, DE). Purified total RNA samples with OD 260/280 ratios greater than 1.8 were used for RT-qPCR measurements. Complementary DNA strands were synthesized for genes of interest using an RT2 first-strand synthesis kit (Qiagen Inc, Valencia, CA). Five hundred nanograms of total RNA was used from each lysate for each first-strand synthesis reaction. Expression levels for specific genes of interest were measured using custom RT2 Profiler RT-PCR arrays (Qiagen Inc, Valencia, CA) and a Bio-Rad CFX96 RT-PCR detection system (Hercules, CA). Statistical analysis of RT-qPCR threshold cycle data was carried out with the web-based RT2 Profiler PCR Array Data Analysis Suite version 3.5 (Qiagen Inc, Valencia, CA) according to published guidelines.[51]

### Adult rat ventricular muscle strip measurements of inotropic response to $CaCl_2$ and isoproterenol

Experiments on isolated adult rat muscle strips were conducted in accordance with the GlaxoSmithKline Policy on the Care, Welfare and Treatment of Laboratory Animals and were reviewed by the IACUC at GlaxoSmithKline. Male Sprague Dawley rats (350–500 g) were anesthetized via inhalation of isoflurane (5% in $O_2$) and euthanized by cervical dislocation. The heart was removed and placed in cold (4°C), oxygenated (95%$O_2$:5%$CO_2$) Krebs buffer containing 10 μU/mL insulin and the following (mM): NaCl, 112.0; KCl, 4.7; $KH_2PO_4$, 1.2; $MgSO_4$, 1.2; $CaCl_2$, 2.5; $NaHCO_3$, 25.0; dextrose, 11.0 (pH 7.4). Right ventricular tissue was excised, cut into strips (approximately 2 mm wide by 12 mm long) and suspended in 10 mL organ baths containing Krebs–Henseleit buffer maintained at 30°C and aerated with 95%$O_2$:5%$CO_2$ (pH 7.4). Changes in isometric force were measured under 1.0 g resting tension using force–displacement transducers and recorded using Chart 5.0 software (AD Instruments, Colorado Springs, CO). The ventricular strips were suspended and stimulated using Radnoti cardiac point stimulating electrodes at 20–30 V for 15 ms with a frequency of 0.3 Hz. After a 60 min equilibration period, 5 mM $CaCl_2$ was added to the tissue bath and the increase in contractility was allowed to plateau (~5 min). Following washout, $CaCl_2$ inotropic response was measured using cumulative 1.5 log concentrations starting at 0.05 mM and ending at 10 mM. After a final washout, cumulative 1.0 log concentrations of isoproterenol (Sigma Aldrich, St. Louis, MO) were administered every 5 min, starting at a concentration of $1e^{-10}$ M and ending with a concentration of $1e^{-4}$ M. Concentration–response curve analysis was performed using a four parameter logistic regression model

$$y = \min + \frac{\max - \min}{1 + \left(\frac{x}{EC_{50}}\right)^{-\text{Hillslope}}} \quad (3)$$

where $EC_{50}$ is the $x$ value for the point on the curve that is halfway between the min and max parameters, which represents the half-maximal effective concentration. The Hill slope is defined as the slope of the curve at its midpoint, where large values represent a steep curve and small values represent a shallow curve. Statistical and concentration–response curve analysis were performed using SigmaPlot 12.0 (Systat Software, Inc., San Jose, CA).

### Neonatal rat MTF measurement of inotropic response to isoproterenol

The contractile response of anisotropic engineered myocardium to increasing concentrations of the β-adrenergic agonist isoproterenol was measured as follows. A 100 mM stock solution of isoproterenol (Sigma Aldrich, St. Louis, MO) containing 110 μM ascorbic acid (Sigma Aldrich, St. Louis, MO) and 45 μM EDTA (Sigma Aldrich, St. Louis, MO) was prepared in Tyrode's solution and stored at −20°C. Working concentrations were prepared fresh for each experiment by serial 10-fold dilution and kept on ice and protected from light during experiments. MTF chips with anisotropic engineered myocardium were prepared and contractile stress generation was measured as described above. Base line recordings of contractile stress were captured after pacing the films at 2 Hz in 37°C Tyrode's solution for 10 min. The engineered tissues were exposed to concentrations of isoproterenol ranging from $1e^{-10}$ to $1e^{-4}$ M by cumulative addition of 1.0 log concentrations every 5 min according to the procedure used for isolated adult rat muscle strips described above. Statistical and concentration–response curve analysis were performed as described above for adult rat isolated muscle strip data.

## Results

### Fabrication of anisotropic engineered myocardium using micro-contact printed ECM guidance cues

Previous work has shown that extracellular boundary cues provided to isolated cardiac myocytes by micro-contact printed ECM patterns guide myofibril assembly in a predictable and reliable manner.[37,38] Moreover, the architecture adopted by cardiac myocytes cultured on micro-contact printed ECM patterns has been shown to influence both $Ca^{2+}$ dynamics[40] and contractility[41,52] in engineered myocardium. We hypothesized that these micro-contact printed ECM patterns could be used to fabricate engineered myocardium that mimics *in vivo* myocardium. To examine the relationship between tissue architecture and *in vitro* maturation of engineered myocardium, we used micro-contact printing to fabricate cell culture substrates with ECM patterns designed to promote the adoption of elongated cellular morphology and parallel myocyte alignment that typifies *in vivo* myocardium (Figure 1(a)). For comparison, we cultured isolated cardiac myocytes on substrates coated with a uniform layer of FN, in the manner typically used for *in vitro* studies (*In vitro* Iso; Figure 1(b)i), that provided no specific geometric guidance cues to the cells (Figure 1(b)ii). We designed two ECM patterns that presented cultured cardiac myocytes with guidance cues to drive their self-organization into aligned tissues. ECM patterns consisting of 15 μm wide lines of FN spaced 15 μm apart (*In vitro* Lines; Figure 1(c)i) were created to simulate areas of the myocardium where embedded non-muscle structures, such as blood vessels, are physically adjacent to cardiac myocytes and influence their organization.[41] This ECM pattern gave rise to thin bands of parallel myocardial fibers with few transverse connections (Figure 1(c)ii). However, the spacing in between these linear constructs did not give rise to engineered myocardium that accurately recapitulated the sheet-like architecture of the myocardium, so we designed a second pattern of 15 μm wide lines of FN spaced 2 μm apart (*In vitro* Aniso; Figure 1(d)i) that imposed parallel cellular alignment, while still promoting transverse coupling between neighboring cardiac myocytes (Figure 1(d)ii).

### Engineered myocardium recapitulates the sarcomere organization of adult myocardium

To assess the influence of ECM guidance cues on the myofibril architecture of engineered myocardium, immunofluorescence imaging of sarcomeric α-actinin was used to visualize z-line orientation and to quantify global, tissue-level sarcomere organization as previously described.[37] Isotropic tissues exhibited z-lines organized randomly in several orientations (Figure 2(a)i), with only small regions of localized anisotropy (Figure 2(a)ii). In contrast, the *In vitro* Lines directed the cardiac myocytes to grow on FN lines just wide enough for them to attach to the substrate end to end and form parallel arrays of muscle fibers (Figure 2(a)iii), imposing a high degree of parallel sarcomere alignment (Figure 2(a)iv). Similarly, the *In vitro* Aniso engineered

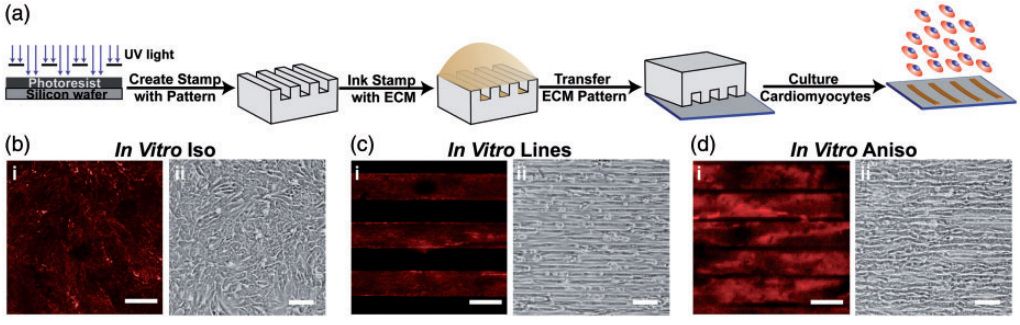


**Figure 1** Controlling the tissue architecture of engineered myocardium using ECM guidance cues. (a) The architecture of engineered cardiac tissues was controlled by micro-contact printing the ECM protein fibronectin (FN) into the desired pattern. Three distinct ECM patterns were chosen for this study to assess the contribution of tissue architecture to the maturation of engineered myocardium *in vitro*. (b) *In Vitro* Iso: coverslips coated uniformly with FN (i), gave rise to monolayers of randomly oriented cardiomyocytes (ii). (c) *In Vitro* Lines: micro-contact printed 15 μm wide FN lines spaced 15 μm apart (i) produced linear arrays of highly aligned cardiac myocytes (ii). (d) *In Vitro* Aniso: micro-contact printed 15 μm wide FN lines spaced 2 μm apart (i) produced confluent anisotropic sheets of cardiac myocytes (ii). For panels bi, ci, di, scale bars = 10 μm. For panels bii, cii, dii, scale bars = 100 μm

myocardium (Figure 2(a)v) also exhibited a high degree of uniaxial, parallel z-line alignment (Figure 2(a)vi). To assess how closely the architecture of our engineered myocardium recapitulated the *in vivo* myocardium, sarcomeric α-actinin immunofluorescence imaging was performed on longitudinal sections taken through the adult rat ventricular myocardium (Figure 2(a)vii). These micrographs revealed a high degree of uniaxial z-line organization, similar to that observed in the *In vitro* Line and *In vitro* Aniso engineered myocardium (Figure 2(a)viii). To quantitatively compare the differences in global z-line organization between the different conditions, custom image processing software was used to measure the orientation angles of the z-lines observed in the α-actinin micrographs and use those angles to calculate the Orientational Order Parameter (OOP) for each tissue architecture.[41,47] The OOP can take on a value between zero, representing completely random organization, and one, representing perfect parallel alignment. These values allowed statistical comparisons of global sarcomere alignment between engineered myocardium and the histological sections of adult rat myocardium (Figure 2(b)). The sarcomeric OOP of the *In vitro* Iso engineered tissues was close to zero, corresponding to the large distribution of z-line orientation angles observed in these samples. In contrast, the sarcomeric OOP values for the *In vitro* Lines and *In vitro* Aniso engineered myocardium were significantly higher ($p < 0.05$) than those observed in the *In vitro* Iso tissues. Moreover, the adult rat heart tissue sections exhibited a sarcomeric OOP value that closely matched the OOP values for the *In vitro* Lines and *In vitro* Aniso engineered myocardium. Taken together, these results show that the degree of parallel sarcomere alignment imposed by anisotropic ECM boundary conditions recapitulated the degree of sarcomere alignment observed in the ventricular myocardium.

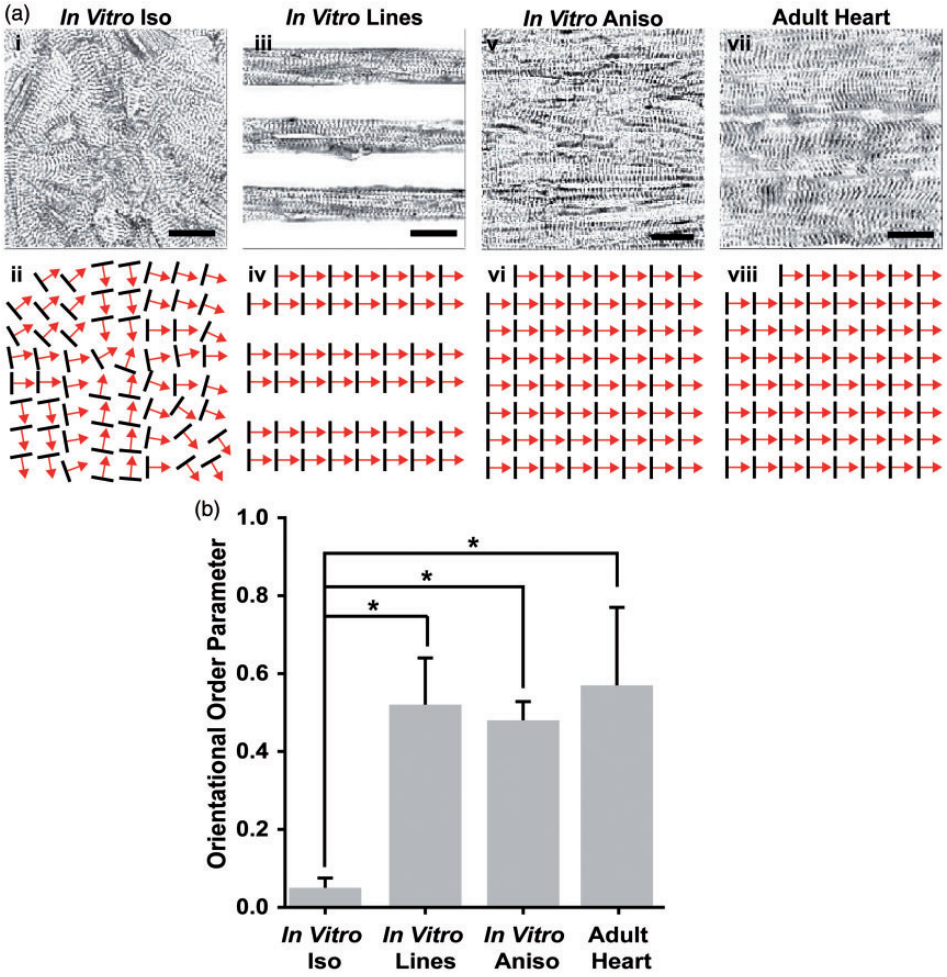


**Figure 2** Comparison of global sarcomere alignment in engineered and adult myocardium. (a) Assessment of sarcomeric α-actinin fluorescence micrographs of isotropic samples (i) revealed random z-line organization as illustrated in the schematic below (ii). In contrast, α-actinin micrographs of cardiac myocytes cultured on 15 μm wide FN lines spaced 15 μm apart (iii), displayed the high degree of parallel alignment expected from the ECM patterning, as illustrated in this schematic (iv). The z-lines of cardiomyocytes cultured on 15 μm wide FN lines spaced 2 μm apart (v) also displayed the degree of parallel z-line alignment expected from this ECM pattern, as illustrated in this schematic (vi). Comparison of micro-contact printed engineered myocardium to the z-line organization observed in histological sections of the adult rat ventricular myocardium (vii) reveals a similar level of global sarcomere alignment as illustrated in this schematic (viii). (b) Statistical comparison of global sarcomere alignment quantified using the Orientational Order Parameter revealed that the anisotropic engineered myocardium showed similar levels of alignment to the adult rat ventricular myocardium. n = 3 tissues for *In Vitro* Iso, *In Vitro* Lines, and *In Vitro* Aniso; n = 4 ventricles for Adult Heart. Scale bars = 10 μm. * = $P < 0.05$ versus *In vitro* Iso

### Tissue architecture influences contractility in engineered myocardium

The relationship between tissue architecture and contractility was assessed in our engineered myocardium using the MTF contractility assay.[43,44,53] These MTF constructs consisted of a layer of cardiac myocytes cultured on top of thin, rectangular elastic films attached to a glass coverslip. Once the free edges of the MTFs were released from the coverslip, shortening of the cardiac myocytes during each contraction cycle caused the films to bend up out of the plane of the coverslip, with the MTFs lying flat against the substrate during diastole (Figure 3(a)i,ii), and at maximum curvature during peak systole (Figure 3(a)iii,iv). High speed imaging of film curvature allowed visualization of the temporal profile of MTF bending and was used to calculate the amount of contractile stress generated by each type of engineered myocardium.[53] *In vitro* Iso tissues exhibited a flat contractile stress profile, indicative of the inability of the randomly organized cardiac myocytes to generate enough uniaxial contractile stress to substantially bend the MTF cantilevers (Figure 3(b)i). In contrast, the more highly aligned *In vitro* Lines (Figure 3(b)ii) and *In vitro* Aniso (Figure 3(b)iii) engineered myocardium exhibited substantially greater contractile force. Statistical comparison of the diastolic and peak systolic stresses generated by the *In vitro* Iso, *In vitro* Lines, and *In vitro* Aniso engineered myocardium revealed that the *In vitro* Lines and *In vitro* Aniso engineered tissues both generated significantly ($p < 0.001$) higher values than the *In vitro* Iso tissues (Figure 3(c)). Comparison of the twitch stress (i.e. the difference between the diastolic and peak systolic stresses) generated by each type of engineered tissue revealed that the *In vitro* Lines and *In vitro* Aniso engineered tissues both generated significantly ($p < 0.001$) higher values than the *In vitro* Iso tissues. Twitch stress values calculated for the adult rat ventricular muscle strips (Adult Heart) were comparable to values measured in the *In vitro* Lines and *In vitro* Aniso engineered myocardium, but significantly ($p < 0.001$) higher than those observed in the *In vitro* Iso tissues (Figure 3(c)). Furthermore, comparison of the auxotonic twitch stress values for the engineered myocardium to isometric contractile stress values reported in the literature for ventricular papillary muscle strips showed that the *In vitro* Lines and *In vitro* Aniso, but not *In vitro* Iso engineered cardiac tissues exhibited values within the same range.[54,55] Taken together, these results show that the anisotropic myofibril architecture imposed by the micropatterned ECM cues gave rise to engineered myocardium with contractile performance comparable to isolated adult rat muscle strips commonly used for studies of cardiac contractility and inotropic response to drug compounds.[57]

### Inotropic response to $CaCl_2$ and isoproterenol in engineered and adult myocardium

A key aspect that distinguishes mature from immature myocardium is inotropic response to changes in

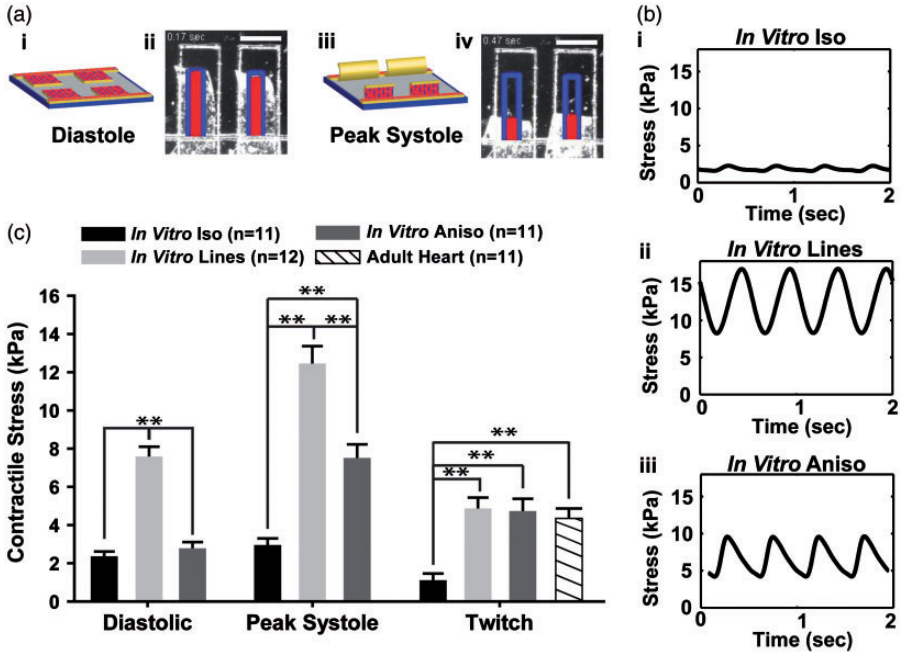


**Figure 3** Measurement and comparison of contractile performance in engineered rat myocardium. (a) Engineered myocardium cultured on MTF cantilevers lay almost flat against the substrate during diastole (i, ii) and curled up out of the plane of the substrate during systolic contraction (iii, iv), scale bars = 1 mm. (b) High speed video recording allows calculation of stress traces during contraction cycles. Representative stress traces for engineered tissues *In Vitro* Iso (i), *In Vitro* Lines (ii), *In Vitro* Aniso (iii). (c) Statistical comparison of diastolic (rest), peak systolic (maximum contraction), and twitch (difference between diastolic and peak systolic) stresses generated by engineered myocardium with isotropic (*In Vitro* Iso) and anisotropic (*In Vitro* Lines, *In Vitro* Aniso) sarcomere organization. Twitch stress from baseline measurements of adult rat muscle strip contractility (Adult Heart) were calculated and compared to values calculated for engineered myocardium. *In Vitro* Lines, and *In Vitro* Aniso engineered myocardium demonstrated twitch stress values within the range reported for adult myocardium[54,55,56] (*In vitro* Iso: n = 11 films, #chips = 3; *In Vitro* Lines: n = 12 films, #chips = 3; *In Vitro* Aniso: #chips = 3; n = 11 films, Adult Heart: n = 11 muscle strips), **=$P < 0.001$ versus *In vitro* Iso

extracellular $Ca^{2+}$ concentration and adrenergic agonists.[58–60] Isolated preparations of adult ventricular muscle are commonly used to measure the contractile response of the myocardium to drug compounds,[61] and the response of the rat myocardium to β-adrenergic stimulation has been studied extensively,[59,62–64] making it a good candidate for determining whether the engineered cardiac tissues recapitulate the contractile response profile observed in isolated heart tissue preparations. We exposed adult rat muscle strips and engineered myocardium to increasing concentrations of $CaCl_2$ ranging from 0.05 to 10 mM to compare their contractile response to changes in extracellular $Ca^{2+}$ concentration (Figure 4(a)). Adult rat muscle strips (Adult Heart) exhibited increasing contractile force as $Ca^{2+}$ concentration increased, demonstrating a half maximal effective concentration ($EC_{50}$) of 3 mM (Figure 4(b)). In comparison, the *In Vitro* Lines (Figure 4(c)) and *In Vitro* Aniso (Figure 4(d)) engineered myocardium also exhibited increasing contractile stress generation in response to increasing $Ca^{2+}$ concentrations, though to a lesser magnitude than the adult rat muscle strips, demonstrating $EC_{50}$ concentrations of 7 and 5 mM, respectively.

To assess the inotropic response of our engineered myocardium to β-adrenergic stimuli, we exposed them to the β-adrenergic agonist isoproterenol in concentrations ranging from 100 pM to 100 μM and measured their contractility using the MTF platform (Figure 4(e)). The concentration–response profile of muscle strips isolated from the ventricular myocardium of adult rats was also measured to provide a comparison for assessing the physiological response of the *In vitro* Lines and *In vitro* Aniso engineered myocardium to isoproterenol exposure. In agreement with previously reported studies,[59,60,63] adult rat ventricular muscle strips (Adult Heart) exhibited a half maximal effective concentration ($EC_{50}$) of 35 nM with respect to their contractile response to isoproterenol (Figure 4(f)). In comparison, neonatal rat cardiac myocytes cultured on 15 μm wide lines of FN spaced 15 μm apart (*In vitro* Lines) exhibited an $EC_{50}$ of 200 nM (Figure 4(g)), and those cultured on 15 μm wide lines of FN spaced 2 μm apart (*In vitro* Aniso) exhibited an $EC_{50}$ of 143 nM (Figure 4(h)). Although statistical comparison of the $EC_{50}$ values calculated for the engineered and adult rat myocardium did not reveal a significant difference between them (one-way ANOVA, $P = 0.96$), the *In vitro* Lines and *In vitro* Aniso nonetheless exhibited an order of magnitude less sensitivity to isoproterenol than the adult rat ventricular muscle strips. A substantial increase in contractile response variability was observed at isoproterenol concentrations greater than 100 nM in the engineered myocardium conditions, potentially due to inherent variation in the maximal contractile rate between preparations. It has been previously shown that engineered tissues comprised of neonatal rat cardiomyocytes exhibit limited inotropic response to isoproterenol at concentrations of 1 μM and above.[10] Taken together, these results indicate that although we observed a trend toward positive inotropic response in our engineered myocardium, mimicking the laminar architecture of the *in vivo* myocardium is just one of many microenvironmental cues necessary to recapitulate the inotropic response profile of adult heart muscle tissue.

### Comparison of engineered and adult rat myocardium gene expression profiles

Alterations in cardiomyocyte shape mediated by cytoskeletal remodeling have been shown to influence gene expression *in vivo* during the early stages of prenatal cardiac morphogenesis[65–67] with distinct, chamber-specific expression profiles as heart development progresses.[68,69] We postulated that recapitulating the cellular architecture and parallel alignment observed in the myocardium *in vivo* may influence the expression of cardiac genes *in vitro* toward expression levels observed in postnatal cardiac myocytes. To test this hypothesis, we performed RT-qPCR measurements of the expression of a panel of genes associated with myocardial development and function (Table S1) on engineered and adult rat myocardium. We calculated fold change for the engineered myocardium samples versus the adult heart expression values, and used Gene Expression Dynamics Inspector (GEDI)[70] software to visually compare and contrast how closely the global expression profiles of the *In Vitro* Iso (Figure 5(a)i), *In Vitro* Lines (Figure 5(a)ii), and *In Vitro* Aniso (Figure 5(a)iii) engineered tissues match the profile of the mature myocardium. GEDI uses a self-organizing map algorithm to cluster genes according to expression profile and maps them to a mosaic grid of user-defined size. Each tile in the mosaic is colored according to the centroid fold change value of the genes that were clustered into that tile to create a visual map of the global expression profile for each type of engineered tissue versus the adult myocardial tissue. Comparison of the GEDI mosaics revealed clusters of genes that exhibited differential expression profiles between the In *Vitro* Iso (Figure 5(a)i) and *In Vitro* Aniso (Figure 5(a)iii) conditions. Hierarchical clustering analysis of the *In Vitro* Iso, *In Vitro* Lines, *In Vitro* Aniso, and adult heart gene expression profiles (Figure 5(b)) revealed that the adult heart expression profile was largely distinct from those of the engineered myocardium samples, with respect to a number of myofibril and ion channel genes. Particularly, potassium ion channel subunit genes associated with voltage-gated (i.e. *Kcna5, Kcnd2*) and inwardly rectifying (i.e. *Kcna5, Kcnd2*) potassium channels exhibited greater than 20-fold down-regulation in the engineered myocardium relative to the adult rat myocardium (Figure 5(a)i–iii). However, similar expression levels were observed for a number of integrin (i.e. *Itga4, Itga5, Itgb3*) and voltage-gated $Ca^{2+}$ channel (i.e. *Cacna1g, Cacna1h, Cacna1d*) genes with the *In Vitro* Lines and *In Vitro* Aniso engineered myocardium. It is well established that in the rodent myocardium, β-myosin heavy chain (β-MHC) is the predominant MHC isoform expressed during prenatal development, and that expression levels switch to favor α-MHC postpartum.[71] Thus, we calculated the ratio of α-/β-MHC for our adult heart and engineered myocardium as a metric of maturation for the *In Vitro* Iso, *In Vitro* Lines, and *In Vitro* Aniso samples (Figure 5(c)). The *In Vitro* Lines engineered myocardium exhibited an α-/β-MHC ratio closest to the Adult Heart samples, but no significant differences were measured between any of the samples. The ventricular isoform of myosin light chain (*Myl2*) also serves as a marker of ventricular myocardial development,[68] thus we examined the expression level of this

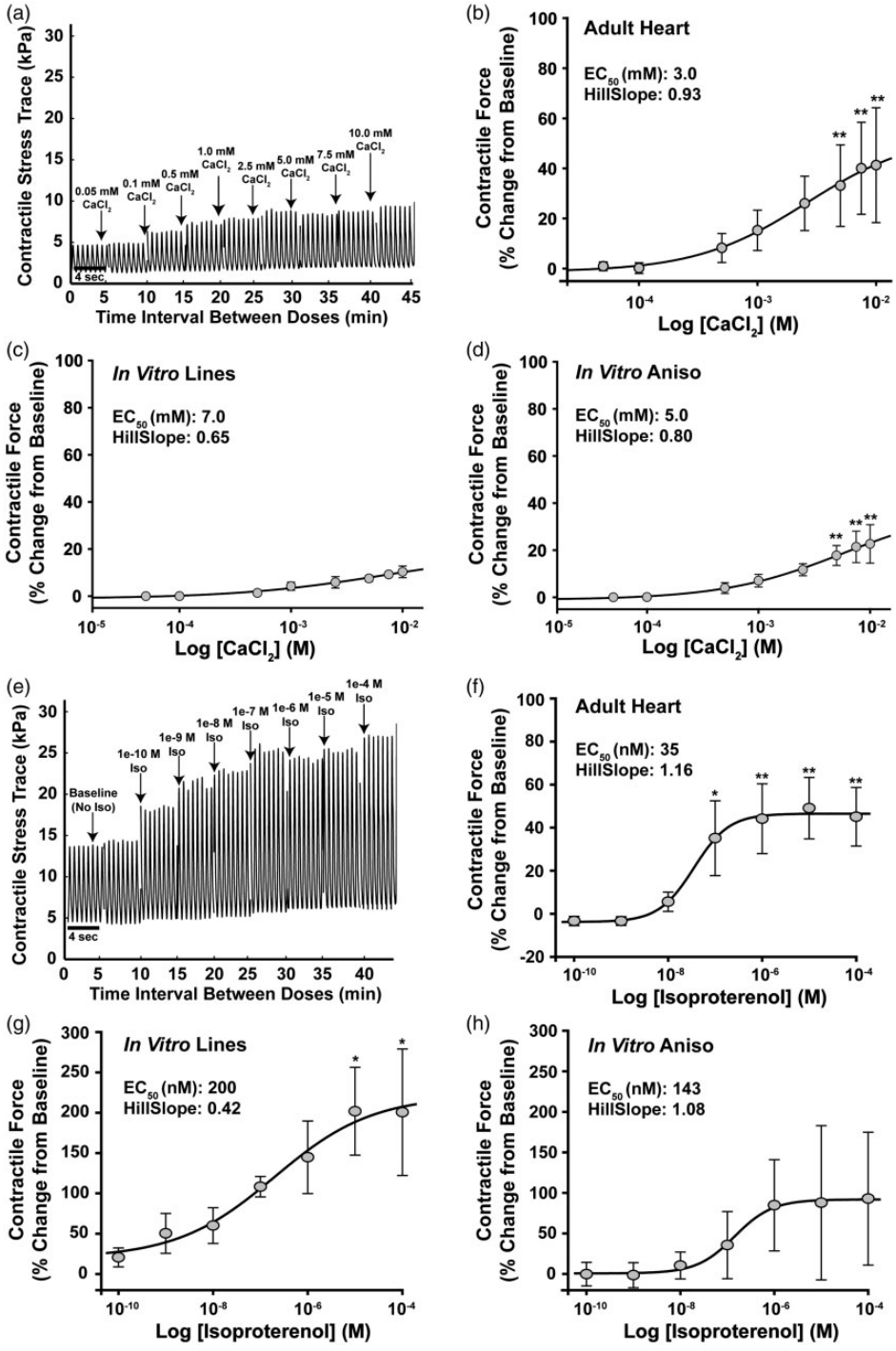


**Figure 4** Measurement and comparison of inotropic response to $CaCl_2$ and isoproterenol in engineered and adult rat myocardium. (a) Example stress trace from MTF contractility measurements illustrating the Calcium chloride ($CaCl_2$) concentration response protocol used to compare the inotropic response profiles of engineered and adult rat myocardium. $CaCl_2$ was administered cumulatively over 5 min intervals to achieve bath concentrations ranging from 0.05 to 10 mM, and contractile stress measurements were recorded at each concentration. (b) Percent change from baseline contractile response profile of ventricular muscle strips isolated from adult rats (Adult Heart) to increasing $CaCl_2$ concentration, $EC_{50} = 3$ mM, n = 6 muscle strips. (c) Percent change from baseline contractile response profile of engineered myocardium comprised of neonate rat cardiac myocytes cultured on 15 μm wide FN lines spaced 15 μm apart (*In Vitro* Lines) to increasing $CaCl_2$ concentration, $EC_{50} = 7$ mM, n = 9 MTFs, #chips = 2. (d) Percent change from baseline contractile response profile of engineered myocardium comprised of neonate rat cardiac myocytes cultured on 15 μm wide FN lines spaced 2 μm apart (*In Vitro* Aniso) to increasing $CaCl_2$ concentration, $EC_{50} = 5$ nM, n = 15 MTFs, #chips = 3. (e) Example stress trace from MTF contractility measurements illustrating the Isoproterenol (Iso) concentration–response protocol used to compare the inotropic response profiles of engineered and adult rat myocardium. Baseline contractile stress measurements were recorded for 10 min, then Iso concentrations ranging from $10^{-10}$ to $10^{-4}$ M were administered in 5 min intervals and recordings of contractile force were taken for each muscle construct. (f) Percent change from baseline contractile response profile of ventricular muscle strips isolated from adult rats (Adult Heart) to isoproterenol exposure, $EC_{50} = 35$ nM, n = 4 muscle strips. (g) Percent change from baseline contractile response profile of engineered myocardium comprised of neonate rat cardiac myocytes cultured on 15 μm wide FN lines spaced 15 μm apart (*In Vitro* Lines) to isoproterenol exposure, $EC_{50} = 200$ nM, n = 13 MTFs, #chips = 4. (h) Percent change from baseline contractile response profile of engineered myocardium comprised of neonate rat cardiac myocytes cultured on 15 μm wide FN lines spaced 2 μm apart (*In Vitro* Aniso) to Iso exposure, $EC_{50} = 143$ nM, n = 15 MTFs, #chips = 4. * = $P < 0.05$ versus baseline, ** = $P < 0.001$ versus baseline. Data presented as mean ± SEM

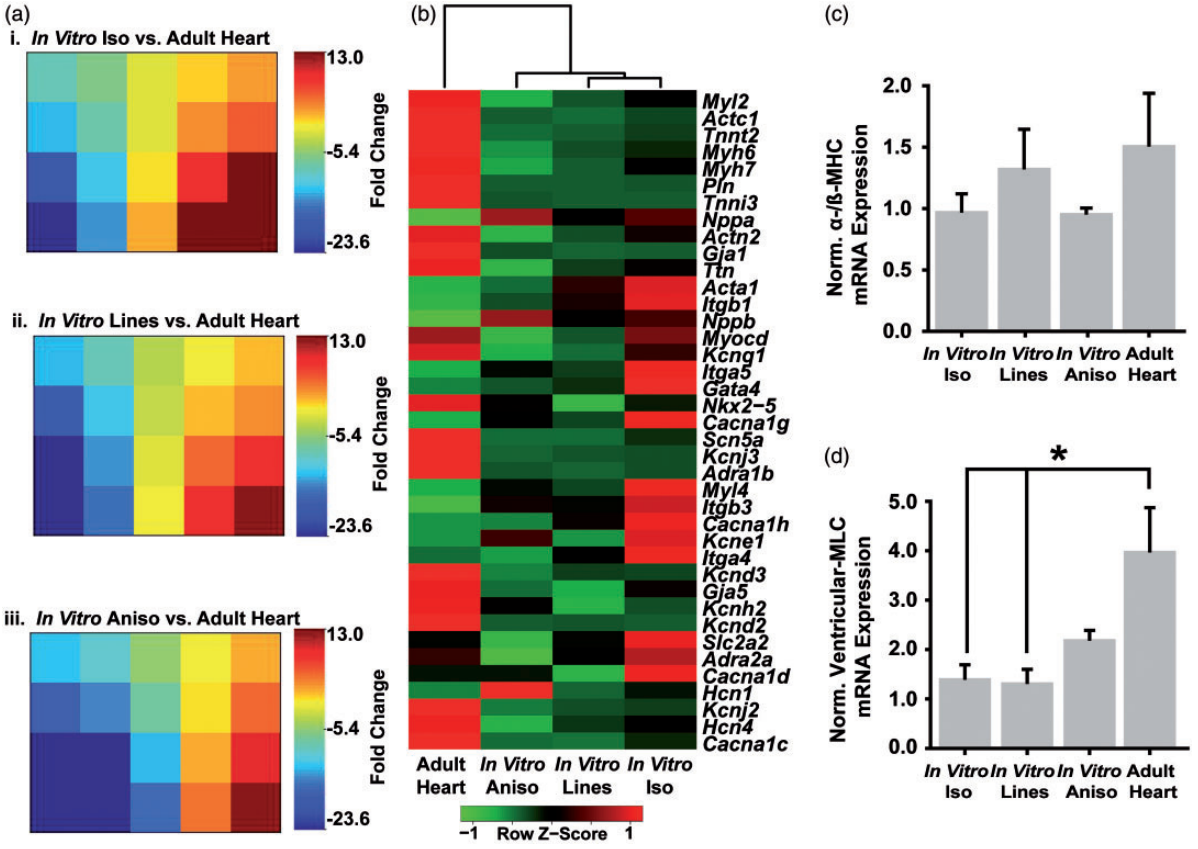


**Figure 5** Comparison of gene expression profiles in engineered and adult rat myocardium. RT-qPCR measurements were made for a panel of genes associated with myocardial development (Supp. Table S1) on *In Vitro* Iso, *In Vitro* Lines, and *In Vitro* Aniso engineered myocardium, as well as explants from adult rat ventricular tissue. (a) Fold change values were calculated against the Adult Heart tissue for the *In Vitro* Iso (i), *In Vitro* Lines (ii), *In Vitro* Aniso (iii) tissues and analyzed with Gene Expression Dynamics Inspector (GEDI) to visualize global differences in the expression profiles between the engineered myocardium versus *in vivo* myocardium. (b) Heat map illustrating hierarchical clustering of the engineered and *in vivo* myocardial tissue based on mean $2^{-\Delta Ct}$ expression values. (c) α-/β-myosin heavy chain ratio was not significantly different between engineered myocardium and adult myocardium, (d) *In Vitro* Iso and *In Vitro* Lines engineered myocardium samples both exhibited significant differences in ventricular myosin light chain (*MYL2*) expression from Adult Heart tissue explants, whereas the *In Vitro* Aniso samples did not. n = 3 tissues for all samples, * = $P < 0.05$ versus Adult Heart. Data presented as mean ± SEM

gene in each of our engineered tissues and compared it to the expression level in adult left ventricular tissues (Figure 5(d)). Adult rat myocardium exhibited significantly ($P < 0.05$) higher expression of ventricular myosin light chain (*Myl2*) than the *In Vitro* Iso and *In Vitro* Lines tissues. However, the *In Vitro* Aniso engineered myocardium more closely matched the expression level observed in the adult rat heart. Taken together, these results suggest that physical microenvironmental cues provided by patterned ECM influence the expression of myofibril-related genes *in vitro*, but additional cues are needed to fully recapitulate the cardiac gene expression profile of adult myocardium.

## Discussion

In this study, we asked if engineered myocardial tissues designed to mimic the anisotropic architecture of the native myocardium could recapitulate the physiological characteristics of adult heart muscle. *In vivo*, myocardial development is the product of a diverse set of biochemical and mechanical cues that are spatially and temporally choreographed to drive cardiac myocyte maturation and the formation of well-ordered myocardial tissue.[15] The mechanical linkage provided by integrin receptors between the ECM and the cytoskeleton serves as a signaling conduit that has been implicated in regulating a number of biological processes, such as cell spreading and sarcomere formation, over the course of myocardial development.[15,72] The laminar architecture of the myocardium greatly influences its functional performance, and micro-contact printed ECM substrates provide a robust platform for examining this interrelationship. Studies by Rohr *et al.*[32] were the first to show that ECM micro-patterning techniques can be used to create muscle tissue constructs from neonatal rat cardiac myocytes with precisely defined and reproducible cellular morphology and organization. Moreover, they showed that these micro-patterned strands of aligned cardiac myocytes exhibited impulse propagation and anisotropy ratios that closely matched *in vivo* measurements.[35,36,73]

We found that imposing anisotropic tissue architecture via ECM patterning cues influenced the maturation of engineered myocardium comprised of neonatal rat cardiac myocytes toward the adult phenotype. Micro-contact printed ECM was used to direct the self-organization

of neonatal cardiac myocytes into anisotropic sheets of muscle tissue *in vitro*, and we examined their sarcomere organization, contractility, inotropic response to β-adrenergic stimulation, and gene expression profile, to determine the manner in which boundary conditions imposed by the ECM patterns could influence the maturation of engineered myocardium. It has been previously shown that the cell shape and tissue architecture imposed by geometric cues encoded in the ECM directly influence sarcomere organization, calcium transients, conduction velocity, and contractile performance of engineered myocardium.[37–41,74] However, the degree to which these engineered myocardial tissues match the physiological profile of adult ventricular muscle has not been shown. We compared and contrasted a number of important aspects of myocardial tissue form and function between our engineered and adult rat myocardium to gauge their similarity. Comparison of global sarcomere z-line alignment and contractile force generation showed that the engineered anisotropic myocardium (*In vitro* Lines, *In vitro* Aniso) were able to recapitulate the myofibrillar structure–function of the isolated adult rat muscle strips. Previously, we reported that neonatal rat cardiac myocytes cultured on lines of micro-contact printed FN (*In vitro* Lines) exhibited significantly ($P < 0.05$) higher global sarcomere alignment than neonate cardiac myocytes cultured on FN patterns designed to create anisotropic muscle sheets (*In vitro* Aniso), as judged by OOP.[41] We did not observe a statistical difference between these conditions in this study due to improvements in our micro-contact printing procedure for fabricating anisotropic engineered myocardium,[9] and to the analysis software we developed for quantifying global sarcomere alignment[47] that resulted in a slight increase in the mean OOP value for our engineered anisotropic myocardium over what we have shown previously. Additionally, the *In vitro* Lines and *In vitro* Aniso constructs exhibited a trend toward positive inotropic response to the β-adrenergic agonist isoproterenol with $EC_{50}$ values within the same order of magnitude as adult rat ventricular muscle strips. Finally, comparison of gene expression in the anisotropic engineered and adult rat myocardium revealed that a number of key genes in myofibril development, particularly myosin-related genes, demonstrated similar expression profiles that were not recapitulated in the isotropic, randomly organized *in vitro* tissues.

While the anisotropic tissue architecture imposed on neonatal cardiac myocytes demonstrated a limited influence on their maturation state, cell shape is only one of many factors that contribute to the development of cardiac myocytes. Factors such as substrate stiffness,[42] time in culture,[75] electrical stimulation,[76] and biochemical cues[17] have all been shown separately to participate in cardiac myocyte development, but optimal *in vitro* maturation will likely require proper integration of these factors to mimic the spatial and temporal kinetics of normal myocardial development. Identifying the combination of microenvironmental signaling cues that drive optimal cardiac myocyte development *in vitro* is an important design consideration for fabricating engineered myocardium, particularly when human stem cell-derived cardiac myocytes are used as the building blocks for the tissue.[5,77,78] Another limitation of our model system is that it is a two-dimensional monolayer of a relatively homogeneous population of cardiac myocytes that does not recapitulate the three-dimensional architecture or heterotypic cellular demographics of the *in vivo* myocardium. We designed two distinct ECM patterns to simulate the different boundary conditions present in the intact myocardium to study the potential role that these physical cues may play in cardiac development.[26,37] As techniques and materials for fabricating ECM substrates that more closely mimic the three-dimensional architecture of the heart improve,[79,80] it will be of critical importance to understand the hierarchy of boundary conditions that drive not only the self-organization of cardiac myocytes, but also the role that those boundary conditions play in development, in order to design *in vitro* platforms for making clinically relevant measurements of myocardial function for disease modeling and drug testing.[81–83]

The results of this study demonstrate a role for ECM geometric cues in promoting the maturation of developmentally immature neonatal rat cardiac myocytes into engineered myocardium that recapitulate the spatial order of myofibril assembly, contractile performance, and interestingly, the expression profile of key sarcomere genes observed in adult rat ventricular myocardium. Using quantitative image analysis,[47] and the MTF contractility assay,[9,52,53] we were able to compare and contrast the structural and functional properties that emerged in our engineered myocardium with the myofibril organization and contractile strength of the mature isolated ventricular muscle strips that they are meant to replace. Moreover, qPCR measurement of cardiac gene expression profiles in engineered and adult rat ventricular myocardium demonstrated similar *Myl2* expression levels in the *In vitro* Aniso and adult rat myocardium, suggesting a role for physical microenvironmental cues in guiding myocardial development beyond potentiating myofibril global alignment and anisotropic tissue self-assembly. As platforms, such as Organs-on-Chips increasingly rely on immature human stem cell-derived cell types for generating human-relevant mimics of tissue and organ function, the need to understand and incorporate the necessary developmental cues becomes urgent. Taken together, these findings show that ECM-guided tissue architecture is a key aspect of myocardial development *in vitro*.

**Authors' Contributions:** SPS, AG, PQ, DJB, MAE, APN, DK, PHC, and MLM performed experiments; SPS, AG, JPF, and MAE analyzed data; SPS, AG, PQ, JGF, RNW, EH, and KKP interpreted results of experiments; SPS, AG, and APN prepared figures; SPS, AG, and KKP drafted manuscript; KKP approved final version of manuscript; SPS, AG, PQ, JGF, RNW, EH, and KKP conception and design of research.

#### ACKNOWLEDGEMENTS

We would like thank the Harvard Center for Nanoscale Systems (CNS) for use of their microfabrication facilities. The

work presented here was funded by GlaxoSmithKline Pharmaceuticals, as well as the Harvard Materials Research Science and Engineering Center (MRSEC) under NSF award number DMR-1420570. This material is based upon work supported by, or in part by, the U.S. Army Research Laboratory and the U.S. Army Research Office under Contract No. W911NF-12-2-0036. The views and conclusions contained in this document are those of the authors and should not be interpreted as representing the official policies, either expressed or implied, of the Army Research Office, Army Research Laboratory, or the U.S. Government. The U.S. Government is authorized to reproduce and distribute reprints for Government purposes notwithstanding any copyright notation hereon.

## DECLARATION OF CONFLICTING INTERESTS

The author(s) declared no potential conflicts of interest with respect to the research, authorship, and/or publication of this article.

## REFERENCES

1. Burrows MT. Rhythmical activity of isolated heart muscle cells in vitro. *Science* 1912;**36**:90–2
2. Greek R, Menache A. Systematic reviews of animal models: methodology versus epistemology. *Int J Med Sci* 2013;**10**:206–21
3. Eschenhagen T, Eder A, Vollert I, Hansen A. Physiological aspects of cardiac tissue engineering. *Am J Physiol Heart Circ Physiol* 2012;**303**:H133–43
4. Zimmermann WH, Schneiderbanger K, Schubert P, Didie M, Munzel F, Heubach JF, Kostin S, Neuhuber WL, Eschenhagen T. Tissue engineering of a differentiated cardiac muscle construct. *Circ Res* 2002;**90**:223–30
5. Nawroth JC, Parker KK. Design standards for engineered tissues. *Biotechnol Adv* 2013;**31**:632–7
6. Sidorov VY, Samson PC, Sidorova TN, Davidson JM, Lim CC, Wikswo JP. I-Wire Heart-on-a-Chip I: Three-dimensional cardiac tissue constructs for physiology and pharmacology. *Acta Biomater* 2017;**48**:68–78
7. Huebsch N, Loskill P, Deveshwar N, Spencer CI, Judge LM, Mandegar MA, Fox CB, Mohamed TM, Ma Z, Mathur A, Sheehan AM, Truong A, Saxton M, Yoo J, Srivastava D, Desai TA, So PL, Healy KE, Conklin BR. Miniaturized iPS-cell-derived cardiac muscles for physiologically relevant drug response analyses. *Sci Rep* 2016;**6**:24726
8. Mathur A, Loskill P, Shao K, Huebsch N, Hong S, Marcus SG, Marks N, Mandegar M, Conklin BR, Lee LP, Healy KE. Human iPSC-based cardiac microphysiological system for drug screening applications. *Sci Rep* 2015;**5**:8883
9. Agarwal A, Goss JA, Cho A, McCain ML, Parker KK. Microfluidic heart on a chip for higher throughput pharmacological studies. *Lab Chip* 2013;**13**:3599–608
10. Boudou T, Legant WR, Mu A, Borochin MA, Thavandiran N, Radisic M, Zandstra PW, Epstein JA, Margulies KB, Chen CS. A microfabricated platform to measure and manipulate the mechanics of engineered cardiac microtissues. *Tissue Eng Part A* 2012;**18**:910–9
11. Nunes SS, Miklas JW, Liu J, Aschar-Sobbi R, Xiao Y, Zhang B, Jiang J, Masse S, Gagliardi M, Hsieh A, Thavandiran N, Laflamme MA, Nanthakumar K, Gross GJ, Backx PH, Keller G, Radisic M. Biowire: a platform for maturation of human pluripotent stem cell-derived cardiomyocytes. *Nat Methods* 2013;**10**:781–7
12. Thavandiran N, Dubois N, Mikryukov A, Masse S, Beca B, Simmons CA, Deshpande VS, McGarry JP, Chen CS, Nanthakumar K, Keller GM, Radisic M, Zandstra PW. Design and formulation of functional pluripotent stem cell-derived cardiac microtissues. *Proc Natl Acad Sci USA* 2013;**110**:E4698–707
13. Tiburcy M, Didie M, Boy O, Christalla P, Doker S, Naito H, Karikkineth BC, El-Armouche A, Grimm M, Nose M, Eschenhagen T, Zieseniss A, Katschinksi DM, Hamdani N, Linke WA, Yin X, Mayr M, Zimmermann WH. Terminal differentiation, advanced organotypic maturation, and modeling of hypertrophic growth in engineered heart tissue. *Circ Res* 2011;**109**:1105–14
14. McCain ML, Parker KK. Mechanotransduction: the role of mechanical stress, myocyte shape, and cytoskeletal architecture on cardiac function. *Pflugers Arch* 2011;**462**:89–104
15. Sheehy SP, Grosberg A, Parker KK. The contribution of cellular mechanotransduction to cardiomyocyte form and function. *Biomech Model Mechanobiol* 2012;**11**:1227–39
16. Chien KR, Domian IJ, Parker KK. Cardiogenesis and the complex biology of regenerative cardiovascular medicine. *Science* 2008;**322**:1494–7
17. Yang X, Pabon L, Murry CE. Engineering adolescence: maturation of human pluripotent stem cell-derived cardiomyocytes. *Circ Res* 2014;**114**:511–23
18. Torrent-Guasp F, Kocica MJ, Corno AF, Komeda M, Carreras-Costa F, Flotats A, Cosin-Aguillar J, Wen H. Towards new understanding of the heart structure and function. *Eur J Cardiothorac Surg* 2005;**27**:191–201
19. Gerdes AM, Kellerman SE, Moore JA, Muffly KE, Clark LC, Reaves PY, Malec KB, McKeown PP, Schocken DD. Structural remodeling of cardiac myocytes in patients with ischemic cardiomyopathy. *Circulation* 1992;**86**:426–30
20. Carreras F, Ballester M, Pujadas S, Leta R, Pons-Llado G. Morphological and functional evidences of the helical heart from non-invasive cardiac imaging. *Eur J Cardiothorac Surg* 2006;**29**:S50–5
21. Streeter DD Jr, Spotnitz HM, Patel DP, Ross J, Sonnenblick EH. Fiber orientation in the canine left ventricle during diastole and systole. *Circ Res* 1969;**24**:339–47
22. Itasaki N, Nakamura H, Sumida H, Yasuda M. Actin bundles on the right side in the caudal part of the heart tube play a role in dextro-looping in the embryonic chick heart. *Anat Embryol (Berl)* 1991;**183**:29–39
23. Latacha KS, Remond MC, Ramasubramanian A, Chen AY, Elson EL, Taber LA. Role of actin polymerization in bending of the early heart tube. *Dev Dyn* 2005;**233**:1272–86
24. Manasek FJ, Monroe RG. Early cardiac morphogenesis is independent of function. *Dev Biol* 1972;**27**:584–8
25. Manner J. On rotation, torsion, lateralization, and handedness of the embryonic heart loop: New insights from a simulation model for the heart loop of chick embryos. *Anat Rec A Discov Mol Cell Evol Biol* 2004;**278A**:481–92
26. Spach MS, Heidlage JF, Barr RC, Dolber PC. Cell size and communication: role in structural and electrical development and remodeling of the heart. *Heart Rhythm* 2004;**1**:500–15
27. Hooks DA, Trew ML, Caldwell BJ, Sands GB, LeGrice IJ, Smaill BH. Laminar arrangement of ventricular myocytes influences electrical behavior of the heart. *Circ Res* 2007;**101**:e103–12
28. Schroder EA, Wei YD, Satin J. The developing cardiac myocyte - maturation of excitability and excitation-contraction coupling. In: Sideman S, Beyar R, Landesberg A (eds). *Interactive and integrative cardiology*. Oxford: Blackwell Publishing, 2006, pp. 63–75
29. Gerdes AM. Cardiac myocyte remodeling in hypertrophy and progression to failure. *J Card Fail* 2002;**8**:S264–8
30. Huang S, Ingber DE. Shape-dependent control of cell growth, differentiation, and apoptosis: switching between attractors in cell regulatory networks. *Exp Cell Res* 2000;**261**:91–103
31. Geisse NA, Sheehy SP, Parker KK. Control of myocyte remodeling in vitro with engineered substrates. *In Vitro Cell Dev Anim* 2009;**45**:343–50
32. Rohr S, Scholly DM, Kleber AG. Patterned growth of neonatal rat heart cells in culture. Morphological and electrophysiological characterization. *Circ Res* 1991;**68**:114–30
33. Bursac N, Parker KK, Iravanian S, Tung L. Cardiomyocyte cultures with controlled macroscopic anisotropy - A model for functional electrophysiological studies of cardiac muscle. *Circ Res* 2002;**91**:E45–E54

34. Chung C-Y, Bien H, Sobie EA, Dasari V, McKinnon D, Rosati B, Entcheva E. Hypertrophic phenotype in cardiac cell assemblies solely by structural cues and ensuing self-organization. *FASEB J* 2011;**25**:851–62
35. Fast VG, Kleber AG. Microscopic conduction in cultured strands of neonatal rat heart cells measured with voltage-sensitive dyes. *Circ Res* 1993;**73**:914–25
36. Rohr S, Kucera JP, Kleber AG. Slow conduction in cardiac tissue, I: effects of a reduction of excitability versus a reduction of electrical coupling on microconduction. *Circ Res* 1998;**83**:781–94
37. Grosberg A, Kuo PL, Guo CL, Geisse NA, Bray MA, Adams WJ, Sheehy SP, Parker KK. Self-organization of muscle cell structure and function. *PLoS Comput Biol* 2011;**7**:e1001088
38. Bray MA, Sheehy SP, Parker KK. Sarcomere alignment is regulated by myocyte shape. *Cell Motil Cytoskel* 2008;**65**:641–51
39. Kuo PL, Lee H, Bray MA, Geisse NA, Huang YT, Adams WJ, Sheehy SP, Parker KK. Myocyte shape regulates lateral registry of sarcomeres and contractility. *Am J Pathol* 2012;**181**:2030–7
40. Pong T, Adams WJ, Bray MA, Feinberg AW, Sheehy SP, Werdich AA, Parker KK. Hierarchical architecture influences calcium dynamics in engineered cardiac muscle. *Exp Biol Med (Maywood)* 2011;**236**:366–73
41. Feinberg AW, Alford PW, Jin H, Ripplinger CM, Werdich AA, Sheehy SP, Grosberg A, Parker KK. Controlling the contractile strength of engineered cardiac muscle by hierarchal tissue architecture. *Biomaterials* 2012;**33**:5732–41
42. McCain ML, Yuan H, Pasqualini FS, Campbell PH, Parker KK. Matrix elasticity regulates the optimal cardiac myocyte shape for contractility. *Am J Physiol Heart Circ Physiol* 2014;**306**:H1525–39
43. Grosberg A, Alford PW, McCain ML, Parker KK. Ensembles of engineered cardiac tissues for physiological and pharmacological study: heart on a chip. *Lab Chip* 2011;**11**:4165–73
44. Grosberg A, Nesmith AP, Goss JA, Brigham MD, McCain ML, Parker KK. Muscle on a chip: in vitro contractility assays for smooth and striated muscle. *J Pharmacol Toxicol Methods* 2012;**65**:126–35
45. Rodriguez EK, Hoger A, McCulloch AD. Stress-dependent finite growth in soft elastic tissues. *J Biomech* 1994;**27**:455–67
46. Ramasubramanian A, Taber LA. Computational modeling of morphogenesis regulated by mechanical feedback. *Biomech Model Mechanobiol* 2008;**7**:77–91
47. Pasqualini FS, Sheehy SP, Agarwal A, Aratyn-Schaus Y, Parker KK. Structural phenotyping of stem cell-derived cardiomyocytes. *Stem Cell Reports* 2015;**4**:340–7
48. Bray M-AP, Adams WJ, Geisse NA, Feinberg AW, Sheehy SP, Parker KK. Nuclear morphology and deformation in engineered cardiac myocytes and tissues. *Biomaterials* 2010;**31**:5143–50
49. Hamley IW. *Introduction to soft matter: synthetic and biological self-assembling materials* Rev. ed. Chichester, England; Hoboken, NJ: John Wiley & Sons, 2007
50. Volfson D, Cookson S, Hasty J, Tsimring LS. Biomechanical ordering of dense cell populations. *Proc Natl Acad Sci USA* 2008;**105**:15346–51
51. Schmittgen TD, Livak KJ. Analyzing real-time PCR data by the comparative C(T) method. *Nat Protoc* 2008;**3**:1101–8
52. Feinberg AW, Feigel A, Shevkoplyas SS, Sheehy S, Whitesides GM, Parker KK. Muscular thin films for building actuators and powering devices. *Science* 2007;**317**:1366–70
53. Alford PW, Feinberg AW, Sheehy SP, Parker KK. Biohybrid thin films for measuring contractility in engineered cardiovascular muscle. *Biomaterials* 2010;**31**:3613–21
54. Uehata M, Ishizaki T, Satoh H, Ono T, Kawahara T, Morishita T, Tamakawa H, Yamagami K, Inui J, Maekawa M, Narumiya S. Calcium sensitization of smooth muscle mediated by a Rho-associated protein kinase in hypertension. *Nature* 1997;**389**:990–4
55. Lakatta EG, Gerstenblith G, Angell CS, Shock NW, Weisfeldt ML. Prolonged contraction duration in aged myocardium. *J Clin Invest* 1975;**55**:61–8
56. Effron MB, Bhatnagar GM, Spurgeon HA, Ruano-Arroyo G, Lakatta EG. Changes in myosin isoenzymes, ATPase activity, and contraction duration in rat cardiac muscle with aging can be modulated by thyroxine. *Circ Res* 1987;**60**:238–45
57. van den RJ, van BF. Cumulative dose-response curves. I. Introduction to the technique. *Arch Int Pharmacodyn Ther* 1963;**143**:240–6
58. Pillekamp F, Haustein M, Khalil M, Emmelheinz M, Nazzal R, Adelmann R, Nguemo F, Rubenchyk O, Pfannkuche K, Matzkies M, Reppel M, Bloch W, Brockmeier K, Hescheler J. Contractile properties of early human embryonic stem cell-derived cardiomyocytes: beta-adrenergic stimulation induces positive chronotropy and lusitropy but not inotropy. *Stem Cells Dev* 2012;**21**:2111–21
59. Harding SE, Vescovo G, Kirby M, Jones SM, Gurden J, Poole-Wilson PA. Contractile responses of isolated adult rat and rabbit cardiac myocytes to isoproterenol and calcium. *J Mol Cell Cardiol* 1988;**20**:635–47
60. Park MK, Sheridan PH, Morgan WW, Beck N. Comparative inotropic response of newborn and adult rabbit papillary muscles to isoproterenol and calcium. *Dev Pharmacol Ther* 1980;**1**:70–82
61. Murnin M, Lovas S, Allen JM, Murphy RF. Organ/tissue preparations for the assessment of agonist/antagonist activity. *Methods Mol Biol* 1997;**73**:343–52
62. de Gende AO, Alzueta DP, Cingolani HE. Effect of isoproterenol on relation between maximal rate of contraction and maximal rate of relaxation. *Am J Physiol* 1977;**233**:H404–9
63. Siegl PK, McNeill JH. Positive inotropic responses in cardiac muscles: influence of stimulation frequency and species. *Can J Physiol Pharmacol* 1982;**60**:33–40
64. Siegl PK, MacLeod KM, Rodgers RL, McNeill JH. Inotropic responses, cyclic AMP, and time to peak tension in isolated cardiac preparations. *Adv Myocardiol* 1982;**3**:77–85
65. Taber LA, Lin IE, Clark EB. Mechanics of cardiac looping. *Dev Dyn* 1995;**203**:42–50
66. Price RL, Chintanowonges C, Shiraishi I, Borg TK, Terracio L. Local and regional variations in myofibrillar patterns in looping rat hearts. *Anat Rec* 1996;**245**:83–93
67. Srivastava D, Olson EN. A genetic blueprint for cardiac development. *Nature* 2000;**407**:221–6
68. Bruneau BG. Transcriptional regulation of vertebrate cardiac morphogenesis. *Circ Res* 2002;**90**:509–19
69. Ng SY, Wong CK, Tsang SY. Differential gene expressions in atrial and ventricular myocytes: insights into the road of applying embryonic stem cell-derived cardiomyocytes for future therapies. *Am J Physiol Cell Physiol* 2010;**299**:C1234–49
70. Eichler GS, Huang S, Ingber DE. Gene Expression Dynamics Inspector (GEDI): for integrative analysis of expression profiles. *Bioinformatics* 2003;**19**:2321–2
71. Mahdavi V, Lompre AM, Chambers AP, Nadal-Ginard B. Cardiac myosin heavy chain isozymic transitions during development and under pathological conditions are regulated at the level of mRNA availability. *Eur Heart J* 1984;**5**:181–91
72. Du AP, Sanger JM, Sanger JW. Cardiac myofibrillogenesis inside intact embryonic hearts. *Dev Biol* 2008;**318**:236–46
73. Fast VG, Kleber AG. Anisotropic conduction in monolayers of neonatal rat heart cells cultured on collagen substrate. *Circ Res* 1994;**75**:591–5
74. Parker KK, Tan J, Chen CS, Tung L. Myofibrillar architecture in engineered cardiac myocytes. *Circ Res* 2008;**103**:340–2
75. McCain ML, Agarwal A, Nesmith HW, Nesmith AP, Parker KK. Micromolded gelatin hydrogels for extended culture of engineered cardiac tissues. *Biomaterials* 2014;**35**:5462–71
76. Sathaye A, Bursac N, Sheehy S, Tung L. Electrical pacing counteracts intrinsic shortening of action potential duration of neonatal rat ventricular cells in culture. *J Mol Cell Cardiol* 2006;**41**:633–41
77. Tay CY, Yu H, Pal M, Leong WS, Tan NS, Ng KW, Leong DT, Tan LP. Micropatterned matrix directs differentiation of human mesenchymal stem cells towards myocardial lineage. *Exp Cell Res* 2010;**316**:1159–68
78. Jacot JG, Kita-Matsuo H, Wei KA, Vincent Chen HS, Omens JH, Mercola M, McCulloch AD. Cardiac myocyte force development during differentiation and maturation. *Ann NY Acad Sci* 2010;**1188**:121–7

79. Murphy SV, Atala A. 3D bioprinting of tissues and organs. *Nat Biotechnol* 2014;**32**:773–85
80. Mosadegh B, Xiong G, Dunham S, Min JK. Current progress in 3D printing for cardiovascular tissue engineering. *Biomed Mater* 2015;**10**:034002
81. Stoehr A, Neuber C, Baldauf C, Vollert I, Friedrich FW, Flenner F, Carrier L, Eder A, Schaaf S, Hirt MN, Aksehirlioglu B, Tong CW, Moretti A, Eschenhagen T, Hansen A. Automated analysis of contractile force and Ca2+ transients in engineered heart tissue. *Am J Physiol Heart Circ Physiol* 2014;**306**:H1353–63
82. Bhatia SN, Ingber DE. Microfluidic organs-on-chips. *Nat Biotechnol* 2014;**32**:760–72
83. Capulli AK, Tian K, Mehandru N, Bukhta A, Choudhury SF, Suchyta M, Parker KK. Approaching the in vitro clinical trial: engineering organs on chips. *Lab Chip* 2014;**14**:3181–6